Available online at www.sciencedirect.com
SCIENCE DIRECT®
Optik 117 (2006) 72–76
Optik Optics
www.elsevier.de/ijleo

Growth and optical properties of Mg, Fe Co-doped $LiTaO_3$ crystal

Shuangquan Fang, Decai Ma, Tao Zhang, Furi Ling, Biao Wang*

Electro-Optics Technology Center, Harbin Institute of Technology, Harbin 150001, China

Received 14 January 2005; accepted 20 April 2005

Abstract

Mg, Fe double-doped $LiTaO_3$ and $LiNbO_3$ crystals have been grown by Czochralski method. The optical properties were measured by two-beam coupling experiments and transmitted facula distortion method. The results showed that the photorefractive response speed of Mg:Fe:$LiTaO_3$ was about three times faster than that of Fe:$LiTaO_3$, whereas the photo-damage resistance was two orders of magnitude higher than that of Fe:$LiTaO_3$. In this paper, site occupation mechanism of impurities was also discussed to explain the high photo-damage resistance and fast response speed in Mg:Fe:$LiTaO_3$ crystal.

Keywords: Mg:Fe:$LiTaO_3$ crystal; Exponential gain coefficient; Diffraction efficiency; Response speed; Photo-damage resistance

1. Introduction

Lithium tantalate ($LiTaO_3$, LT) single crystal is one of the promising ferroelectric materials applied in lots of fields, i.e., piezoelectric, electro-optic, surface acoustic wave, waveguide and nonlinear optical devices [1–7]. LT presents the same crystalline structure (trigonal system, 3 m point cluster) as that of lithium niobate ($LiNbO_3$, LN) single crystal, but its melting point (1650 °C) is higher than that of LN (1240 °C), so it is difficult to prepare the LT crystal. In addition, the larger band gap of LT (4.6 eV) than that of LN (3.7 eV) also limits its application. Kim et al. [8] thought that photorefractive effect was attributed to the transition metal (TM) impurities and stacking faults caused by nonstoichiometry and deficiency of oxygen in LT crystals, so it can be improved significantly by doping TM ions like Fe, Cu or Mn. Similar to that of LN, in Fe-doped LT crystals, the photoinduced charge transport process can be expressed by the following equation:

$$Fe^{2+} \leftrightharpoons Fe^{3+} + e,$$

where Fe^{2+} ions acted as electron donors and Fe^{3+} ions act as electron traps. Electrons are excited from Fe^{2+} to the conduct band, and then are redistributed because of diffusion, drift and bulk photovoltaic effect. Finally, they are captured by Fe^{3+}; thus, a space charge field builds up and the refractive index is modulated via the electro-optic effect.

Despite excellent photorefractive properties, there are serious disadvantages in Fe-doped LT, e.g., long response time and low photo-damage resistance ability. The so-called "photo-damage" is also a photorefractive effect, which occurs when the crystals are irradiated with high-power laser beams of visible wavelengths. This effect limits its application in nonlinear optical fields. It is well known that doping with Mg [9], Zn [10], In [11] or Sc [12] ions in LN can significantly improve its photo-damage resistance ability. In this work, MgO is added in

*Corresponding author.
E-mail addresses: shqfang@yahoo.com.cn (S. Fang), wangbiao@hit.edu.cn (B. Wang).

0030-4026/$ - see front matter © 2005 Elsevier GmbH. All rights reserved.
doi:10.1016/j.ijleo.2005.06.002

Fe:LT to grow Mg:Fe:LT and experimental results show that the photo-damage resistance ability increased considerably for inducing Mg^{2+} in Fe:LT crystal. In addition, the photorefractive response time of Mg:Fe:LT decreased to a considerable degree in comparison with Fe:LT crystal.

2. Experimental

2.1. Crystal growth and sample preparation

All crystals including Fe:LN, Mg:Fe:LN, Fe:LT and Mg:Fe:LT are grown from congruent melts by the Czochralski (CZ) method using a resistance-heating furnace. All the starting materials MgO, Fe_2O_3, Li_2CO_3, Nb_2O_5 and Ta_2O_5 used to prepare the crystals are 99.99% in purity. All crystals are grown along $\langle 0\,0\,1 \rangle$ direction at a rotating rate of 10–20 rpm and pulling rate of 1–3 mm/h, and axial temperature gradient 30–50 °C. Important crystal growth parameters for both LT and LN are listed in Table 1. After growth, the crystals are annealed to room temperature in air at a rate of 50 °C/h. All the crystals must be polarized to the single domain state before use. Finally, the crystals that polarize are cut into wafers and polished to optical grade.

2.2. Exponential gain coefficient

The photorefractive properties of the crystals were measured by two-beam coupling experiments. Fig. 1 shows the typical light path scheme of two-beam coupling. A weak probe wave (signal beam I_S) and a pump wave (reference beam I_R), both of which originated from Ar^+ laser (wavelength $\lambda = 514.5$ nm), were incident on the samples with polarization direction parallel to the c-axis of the sample. Then, intensive beams coupling occurred and caused the signal beam to gain intensity at the expense of the reference beam. Coupled wave equations can be obtained approximately by using the scalar wave equations with a light wave transmitted in the grating [13], i.e.,

$$\frac{dI_{RT}}{dz} + \Gamma \frac{I_{RT}I_{ST}}{I_{RT} + I_{ST}} + \alpha I_{RT} = 0, \tag{1}$$

$$\frac{dI_{ST}}{dz} + \Gamma \frac{I_{RT}I_{ST}}{I_{RT} + I_{ST}} + \alpha I_{ST} = 0, \tag{2}$$

where I_{RT} and I_{ST} are the transmitted reference and signal beam intensity with coupling, respectively; Γ is the exponential gain coefficient of two-beam coupling; α is the absorption coefficient of the sample. The light intensity ratio m was introduced into

$$m = I_R/I_S. \tag{3}$$

The total incident light intensity was

$$I = I_R + I_S \tag{4}$$

and

$$I_{RT} + I_{ST} = (I_R + I_S)e^{-\alpha L}, \tag{5}$$

where L is the interaction length of the two beams in the crystal. Combining Eqs. (1)–(5), I_{RT} and I_{ST} can be derived:

$$I_{RT} = \frac{Im^{-1}e^{-\alpha L}}{1 + m^{-1}e^{\Gamma L}}, \tag{6}$$

$$I_{ST} = \frac{Im^{-1}e^{(\Gamma-\alpha)L}}{1 + m^{-1}e^{\Gamma L}}. \tag{7}$$

Therefore, when $\Gamma > \alpha$, the signal light can be enlarged at the expense of the pump light. The energy transformation from pump light to signal light can be evaluated by

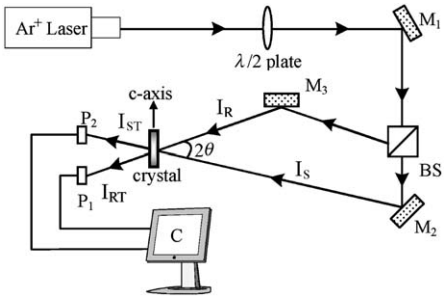

Fig. 1. Light path scheme for two-beam coupling experiment.

Table 1. Crystal growth parameters for both LN and LT crystals

Crystal	$Fe:LiTaO_3$	$Mg:Fe:LiTaO_3$	$Fe:LiNbO_3$	$Mg:Fe:LiNbO_3$
Heating element	SiMo bar	SiMo bar	SiC bar	SiC bar
[MgO] (mol%)	0	6	0	6
[Fe_2O_3] (wt%)	0.03	0.03	0.03	0.03
[Li]/[Ta] (mol ratio)	0.951	0.951	—	—
[Li]/[Nb] (mol ratio)	—	—	0.946	0.946
Wafer size ($a \times b \times c$, mm^3)	$5 \times 2 \times 5$	$5 \times 2 \times 5$	$10 \times 2 \times 10$	$10 \times 2 \times 10$
Growth atmosphere	Air	Air	Air	Air

the exponential gain coefficient Γ, which can be described by the following equation [14]:

$$\Gamma = \frac{1}{L}\ln\left(\frac{I_{ST}}{I'_{ST}}\frac{I'_{RT}}{I_{RT}}\right), \tag{8}$$

where I'_{RT} and I'_{ST} are the transmitted reference and signal beam intensity without coupling. If $I'_{RT} \gg I'_{ST}$, then pump loss can be neglected, i.e., $I'_{RT} = I_{RT}$. Thus, Eq. (8) can be simplified as

$$\Gamma = \frac{1}{L}\ln\frac{I_{ST}(\text{with coupling})}{I'_{ST}(\text{without coupling})}. \tag{9}$$

In this experiment, the diameters of pump and signal light were both 1 mm. The ratio of light intensity was $m = 2550$.

2.3. Diffraction efficiency and response time

Diffraction efficiency and response time were also measured by the two-wave coupling experiment. The experimental setup is shown in Fig. 1. There were two coherent Ar^+ laser beams with identical intensity incident in the sample, in which the c-axis was oriented to be in the incident plane and perpendicular to the bisector of the two beams. The diffraction efficiency η was defined as the ratio between diffractive and transmitting intensities, i.e.,

$$\eta = I'_S/(I'_{ST} + I'_S) \times 100\%, \tag{10}$$

where I'_{ST} is the transmitting intensity of I_S before the grating was built and I'_S is the diffractive intensity of I_S after the grating was built.

Response time τ was defined as the time interval from the initial recording to when diffraction efficiency is reached $\eta_{max}(1 - e^{-1})$, where η_{max} is the maximum of diffraction efficiency.

2.4. Photo-damage resistance

The transmitted beam distortion method was used to evaluate the photo-damage resistance ability of Mg:Fe:$LiTaO_3$ crystal. The experimental setup is shown in Fig. 2. An Ar^+ laser beam (wavelength $\lambda = 488$ nm), whose intensity can be controlled by the adjustable light attenuator and whose polarizing direction was parallel to the c-axis, irradiated to the samples after convergence through the convex lens. The crystal was placed on the focal plane of the lens. The transmitted beam did not distort and the facula was still round under low laser intensity; however, the transmitted facula was smeared and elongated along the c-axis when the laser intensity reached a certain value. The laser power density that just distorted the facula was defined as the photo-damage threshold value R of the crystal. For comparison, samples of Fe:LT, Fe:LN and Mg:Fe:LN were also investigated.

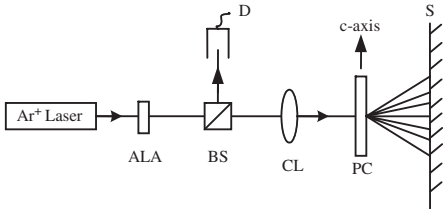

Fig. 2. Experimental setup for photo-damage resistance measurement. ALA, adjustable light attenuator; BS, beam splitter; D, detector; PC, photorefractive crystal; S, screen; CL, convex lens; OS, observation screen.

3. Results and discussion

The experimental results between the exponential gain coefficient Γ and 2θ are shown in Fig. 3, where 2θ is the angle between the reference and signal beams. From the figure, one can observe that the Mg:Fe:LT crystal had a maximal exponential gain coefficient (Γ_{max}) of 18/cm at an angle of about 22°. The intensive light crawling effect that existed in the thinner Mg:Fe:LT sample may be responsible for the higher exponential gain coefficient in a large angle range, similar to that in LN [15].

The experimental results between the diffractive efficiency η and 2θ are given in Fig. 4, which indicates that the diffractive efficiency of Mg:Fe:LT crystal will reach a maximum of 39% at about the angle of 23°.

The optical properties of the samples are listed in Table 2. It can be found from Table 2 that the response speed of the Mg:Fe:LT crystal was about three times higher than that of the Fe:LT crystal and also higher than that of the Mg:Fe:LN crystal. The photo-damage resistances of all the samples are also given in Table 2, which indicates that the photo-damage resistance of the Mg:Fe:LT crystal was two orders of magnitude higher than that of the Fe:LT crystal and was also higher than that of the Mg:Fe:LN crystal. Using Kogelnik's [16]

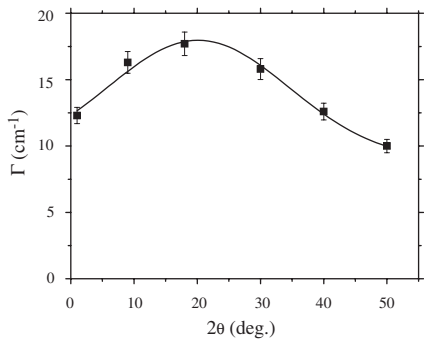

Fig. 3. The experimental results between exponential gain coefficient Γ and 2θ.

formula, i.e., $\eta = \sin^2(\pi L\Delta n/\lambda \cos\theta)$, the photorefractive index change Δn can be obtained; thus, the photo-damage of these crystals can be evaluated quantitatively. The experimental setup is shown in Fig. 1. Two coherent Ar^+ laser beams with identical intensity were incident into the samples at $2\theta = 22^\circ$ in the crystal. The measurement results are given in Table 2.

According to a well-known scalar expression $\Delta n = (n_e^3/2)[Kj_{ph}(\sigma_{ph} + \sigma_d)]$ [17], where n_e is the extraordinary light refractive index, K the electro-optic coefficient, j_{ph} the photogalvanic current, σ_{ph} the photoconductivity and σ_d the dark conductivity, the photorefraction Δn can be obtained to explain photo-damage resistance in the crystals; σ_d can be neglected for $\sigma_d \ll \sigma_{ph}$ in our measurement, whereas the photovoltaic current is almost unvaried, so it is possible to reduce photo-damage by increasing only photoconductivity. Similar the congruent LN crystal, the congruent LT crystal is also Li-deficient ([Li]/[Ta] < 1); therefore, there are a lot of intrinsic defects, such as anti-site tantalum (Ta_{Li}^{4+}) and lithium vacancy (V_{Li}^-) defects, in the LT crystal. In the Fe:LT crystal, Fe^{3+} is the dominant electron acceptor; then a reduced capture section of Fe^{3+} is responsible for the observed increase in photoconductivity. Ta_{Li}^{4+} is the most probable electron acceptor in the congruent LT host, so a reduced Ta_{Li}^{4+} concentration should also result in an increase in photoconductivity if the concentration of Fe^{3+} acceptor is negligible. There should be fewer intrinsic defects in congruent LT than that in congruent LN for [Li]/[Ta] > [Li]/[Nb]. In the congruent LN crystal, threshold concentration of MgO is about 6 mol% [9], so the MgO concentration should have exceeded its threshold in congruent LT doping with 6 mol% MgO. When doping Fe^{3+} in the LT crystal, the role of Ta_{Li}^{4+} is negligible and Fe^{3+} will replace Ta_{Li}^{4+} and Ta^{5+} simultaneously, so photoconductivity is governed by the electron acceptor Fe^{3+}. Similar to the case in the $LiNbO_3$ crystal [18], in the Mg:Fe:LT crystal, Mg^{2+} takes the priority of replacing Ta_{Li}^{4+} and Fe^{3+} will replace Ta_{Li}^{4+} and Ta^{5+} simultaneously. When MgO doping exceeds its threshold in Fe:LT crystal, all Ta_{Li}^{4+} were replaced completely and Fe^{3+} only occupies Ta^{5+} site. So the capture section of Fe^{3+} decreases significantly, which results in increase rapid in photoconductivity. Therefore, Mg(6 mol%):Fe(0.03 wt%):LT presents much higher photo-damage resistance than Fe(0.03 wt%):LT. Likewise, the increased photoconductivity by doping Mg^{2+} in the Fe:LT crystal is also responsible for the fast response speed. Because increased photoconductivity indicated that motion of photoinduced charge carriers would become fast, which made the space charge field form faster, photorefractive response speed increased.

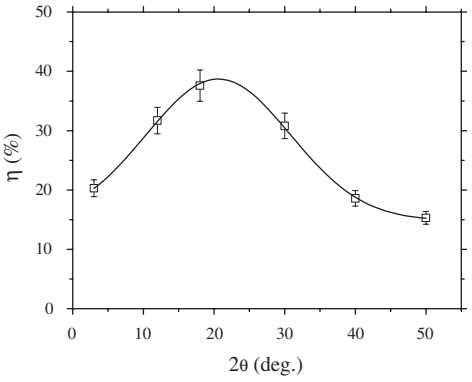

Fig. 4. The experimental results between diffractive efficiency η and 2θ.

4. Conclusion

In conclusion, Mg:Fe:$LiTaO_3$ crystal grown by the CZ method and its optical properties were investigated. It was found that the photorefractive response speed can be greatly improved by doping MgO in Fe:$LiTaO_3$ crystal; moreover, the photo-damage resistance of Mg:Fe:$LiTaO_3$ was two orders of magnitude higher than that of Fe:$LiTaO_3$. Our analysis indicated that the increased photoconductivity was responsible for both fast photorefractive response and high photo-damage resistance in Mg:Fe:$LiTaO_3$ crystal.

Acknowledgements

This work was supported by the National Natural Science Foundation of China (50232030, 10172030), The National Science Foundation of Heilongjiang Province, The Ministry of Science and Technology of China through the High-Tech Program (2001AA31304), and

Table 2. Optical properties of the LT and LN samples

Crystal	Fe:$LiTaO_3$	Mg:Fe:$LiTaO_3$	Fe:$LiNbO_3$	Mg:Fe:$LiNbO_3$
τ (s)	63	19	270	44
R (kW/cm^2)	4.6	553.2	0.8	48.7
η (%)	53	38	68	45
Δn (10^{-5})	6.55	5.34	7.79	5.91

the National Committee of Defense Science And Technology.

Reference

[1] N. Wakatsuki, S. Kudo, M. Chiba, Temperature self-compensated lithium tantalate piezoelectric gyroscope for higher sensitivity and stability, Ultrasonics 38 (2000) 46–50.

[2] I. Reinhard, M. Gabrysch, B. Fischer von Weikersthal, K. Jungmann, G. zu Putlitz, Measurement and compensation of frequency chirping in pulsed dye laser amplifiers, Appl. Phys. B 63 (1996) 467–472.

[3] A. Holm, Q. Stürzer, Y. Xu, R. Weigel, Investigation of surface acoustic waves on $LiNbO_3$, quartz, and $LiTaO_3$ by laser probing, Microelectron. Eng. 31 (1996) 123–127.

[4] I. Sokólska, S. Kück, Optical characterization of Cr^{3+} doped $LiTaO_3$ crystals relevant for laser application, Spectrochim. Acta A 54 (1998) 1695–1700.

[5] V.V. Atuchin, causes of refractive indices changes in He-implanted $LiNbO_3$ and $LiTaO_3$ waveguides, Nucl. Instrum. Methods B 168 (2000) 498–502.

[6] K.-M. Wang, F. Chen, H. Hu, J.-H. Zhang, F. Lu, B.-R. Shi, Q.-M. Lu, C.-Q. Ma, Waveguide formation in $LiTaO_3$ and LiB_3O_5 by keV hydrogen ion implantation, Opt. Commun. 196 (2001) 215–219.

[7] R. Ryf, G. Montemezzani, P. Günter, Y. Furukawa, K. Kitamura, Photorefractive multichannel correlatoir base on stoichiometric $LiTaO_3$, Appl. Phys. B 72 (2001) 737–742.

[8] B.K. Kim, G.Y. Kang, J.K. Yoon, J.H. Ro, The photorefractive effects of Fe and Fe + Ce doped $LiTaO_3$ single crystal, J. Phys. Chem. Solids 61 (2000) 637–646.

[9] Z. Jiguo, J. Jian, W. Zhongkang, Measurement of optically induced refractive-index damage of lithium niobate doped with different concentration of MgO. 11th International Quantum Electronics Conference, New York, IEEE Cat. 80 (1980) 631–635.

[10] T.R. Volk, V.I. Pryalkin, N.M. Rubinina, Optical-damage-resistant $LiNbO_3$:Zn crystal, Opt. Lett. 15 (1990) 996–998.

[11] Y. Kong, J. Wen, H. Wang, New doped lithium niobate crystal with high resistance to photorefraction – $LiNbO_3$: In, Appl. Phys. Lett. 66 (1995) 280–281.

[12] J.K. Yamamoto, K. Kitamura, N. Iyi, S. Kimura, Y. Furukawa, M. Sato, Increased optical damage resistance in Sc_2O_3-doped $LiNbO_3$, Appl. Phys. Lett. 61 (1992) 2156–2158.

[13] P. Günter, Holography, coherent light amplification and optical phase conjugation with photorefractive materials, Phys. Rep. 93 (1982) 199–299.

[14] X. Yue, S. Mendricks, Y. Hu, H. Hesse, D. Kip, Photorefractive Effect in Doped $Pb_5Ge_3O_{11}$ and in $(Pb_{1-x}Ba_x)_5Ge_3O_{11}$, J. Appl. Phys. 83 (1998) 3473–3479.

[15] J. Zhang, W. Sun, H. Zhao, S. Bian, K. Xu, M. Li, Y. Xu, Enhancement of the exponential gain coefficient as a result of the light-fanning effect in thin doped $LiNbO_3$ crystals, Opt. Lett. 18 (1993) 1391–1393.

[16] H. Kogelnik, Coupled wave theory for thick hologram gratings, Bell Syst. Tech. J. 48 (1969) 2909–2947.

[17] Y. Furukawa, K. Kitamura, S. Takekawa, K. Niwa, H. Hatano, Stoichiometric Mg:$LiNbO_3$ as an effective material for nonlinear optics, Opt. Lett. 23 (1998) 1892–1894.

[18] J. Liu, W. Zhang, G. Zhang, Microscopic mechanism of suppressing photorefraction in $LiNbO_3$:Mg, Fe crystals, Solid State Commun. 98 (1996) 523–526.